Received: 27 July 2021 | Accepted: 23 May 2022

DOI: 10.1111/1365-2435.14112

Functional Ecology | BRITISH ECOLOGICAL SOCIETY

RESEARCH ARTICLE

Quantifying within-species trait variation in space and time reveals limits to trait-mediated drought response

Kelly L. Kerr[1] | Leander D. L. Anderegg[2] | Nicole Zenes[1] | William R. L. Anderegg[1]

[1]School of Biological Sciences, University of Utah, Salt Lake City, UT, USA

[2]Department of Ecology, Evolution, and Marine Biology, University of California Santa Barbara, Santa Barbara, CA, USA

Correspondence
Kelly L. Kerr
Email: kelly.kerr@utah.edu

Funding information
David and Lucille Packard Foundation; National Science Foundation, Grant/Award Number: 1747505, 1714972, 1802880, 2003017, 1711243 and 2003205; National Science Foundation GRFP; USDA National Institute of Food and Agriculture, Agricultural and Food Research Initiative Competitive Programme, Ecosystem Services and Agro-ecosystem Management, Grant/Award Number: 2018-67019-27850

Handling Editor: Carlos Perez Carmona

Abstract

1. Climate change is stressing many forests around the globe, yet some tree species may be able to persist through acclimation and adaptation to new environmental conditions. The ability of a tree to acclimate during its lifetime through changes in physiology and functional traits, defined here as its acclimation potential, is not well known.
2. We investigated the acclimation potential of trembling aspen *Populus tremuloides* and ponderosa pine *Pinus ponderosa* trees by examining within-species variation in drought response functional traits across both space and time, and how trait variation influences drought-induced tree mortality. We measured xylem tension, morphological traits and physiological traits on mature trees in southwestern Colorado, USA across a climate gradient that spanned the distribution limits of each species and 3 years with large differences in climate.
3. Trembling aspen functional traits showed high within-species variation, and osmotic adjustment and carbon isotope discrimination were key determinants for increased drought tolerance in dry sites and in dry years. However, trembling aspen trees at low elevation were pushed past their drought tolerance limit during the severe 2018 drought year, as elevated mortality occurred. Higher specific leaf area during drought was correlated with higher percentages of canopy dieback the following year. Ponderosa pine functional traits showed less within-species variation, though osmotic adjustment was also a key mechanism for increased drought tolerance. Remarkably, almost all traits varied more year-to-year than across elevation in both species.
4. Our results shed light on the scope and limits of intraspecific trait variation for mediating drought responses in key southwestern US tree species and will help improve our ability to model and predict forest responses to climate change.

KEYWORDS
climate change, drought response, forest ecophysiology, functional trait, intraspecific trait variation, phenotypic plasticity, *Pinus ponderosa*, *Populus tremuloides*

[Correction added on 14 July 2022, after first online publication: The Supporting Information has been revised.]

1 | INTRODUCTION

Climate change is projected to result in more severe and frequent drought events for many forest ecosystems, particularly in the southwestern United States (Dai, 2013). In recent decades, these southwestern forests have experienced amplified drought conditions (Williams et al., 2020) that resulted in widespread die-offs of multiple tree species (Worrall et al., 2008). To persist under climate change, tree species native to drought-prone regions must be able to acclimate quickly enough to increasing severe drought frequency (Aitken et al., 2008). Indeed, physiological modelling has demonstrated a crucial role for tree acclimation in response to future climate scenarios (Sperry et al., 2019). Drought acclimation is especially important for tree species with clonal propagation, such as aspen, given that rare sexual reproduction via seeds means even more substantial dispersal/migration limitations (Dodd & Douhovnikoff, 2016). However, the ability of a tree to acclimate to new environmental conditions during its lifetime, defined here as its acclimation potential, is not well known yet would greatly improve our ability to model and predict forest responses to climate change (Sperry et al., 2019). Due to the serious consequences of drought-induced tree mortality for forest ecosystems (Adams et al., 2010), it is also vital we improve our ability to forecast drought-induced mortality events which may be possible by linking functional traits to mortality patterns (Anderegg et al., 2019).

Intraspecific variation—which includes both phenotypic plasticity and genetic differences—reflects how diverse distinct populations are within a species (Albert et al., 2010). Intraspecific variation in relevant functional traits that are outcomes of genome-by-environment interactions may enhance tree species' acclimation potential to drought, whereby higher intraspecific variation would indicate that at least some populations within a species may be able to tolerate environmental change (Anderegg, 2015). The extent of phenotypic plasticity and intraspecific variation of functional traits in tree species is not fully understood, but will be critical for understanding tree species' acclimation potentials (Violle et al., 2014). Although determination of phenotypic plasticity is often conducted using common garden experiments to better control the environmental conditions each genotype experiences, this approach is generally not logistically possible with mature forest trees. In addition, most common garden studies that investigate functional traits are conducted using tree seedlings and saplings. Yet estimating phenotypic plasticity in mature forest stands can be achieved by measuring temporal variation in functional traits, where temporal variation in climate conditions generates different environmental conditions and genotype is controlled by measuring the same individual trees over time (Borghetti et al., 2017).

There are various functional traits (i.e. drought response traits) that determine how trees cope with drought stress. These traits encompass aspects of xylem anatomy, hydraulic conductance, leaf morphology and biophysics. In the plant hydraulic continuum, embolisms can form in xylem tissue due to increased tension in the water column during drought, resulting in loss of hydraulic conductance which may eventually lead to hydraulic failure and tree death (Sperry & Tyree, 1988). In the absence of embolisms, tree species with high hydraulic conductivity are more hydraulically efficient and can readily move water from roots to leaves without increasing xylem tension to damaging levels (Maherali et al., 2004). Similarly, tree species with high native leaf area-specific conductivity can provide greater hydraulic support to leaf area while incurring less xylem tension (McCulloh & Sperry, 2005). In addition, tree species with low specific leaf area (leaf area per unit dry mass, SLA) have less water demand per unit leaf mass and are more tolerant to increased xylem tensions (Wright et al., 2004). Tree species with smaller leaf area-to-sapwood area ratios also have less evaporative demand and reduce the xylem tension required to move water to the foliage (Martínez-Vilalta et al., 2009). Furthermore, leaf water potential at the turgor loss point (Ψ_{TLP}) dictates the point when leaves wilt and are no longer able to sustain photosynthetic function, and tree species with more negative values of Ψ_{TLP} have been shown to be more drought tolerant (Bartlett et al., 2012; McGregor et al., 2021). Finally, tree species with high intrinsic water-use efficiency (photosynthetic rate divided by stomatal conductance, often estimated based on leaf carbon isotope discrimination) are typically thought to be better able to maintain carbon fixation under water stress (Ehleringer, 1993).

Here, we investigate the extent of spatial and temporal intraspecific variation in drought response traits to determine the acclimation potential and influence of intraspecific trait variation on drought-induced tree mortality of trembling aspen and ponderosa pine in southwestern Colorado, USA. We measured intraspecific variation in xylem tension and drought response traits across a climate gradient that spanned the distribution limits of each species and three climatically different years to answer the following questions: (a) What is the extent of spatial intraspecific variation in drought response traits?; (b) What is the extent of temporal intraspecific variation in drought response traits?; and (c) Do drought response trait values predict drought-induced tree mortality within species following a severe drought?

2 | MATERIALS AND METHODS

2.1 | Study system

Focal tree species were trembling aspen (*Populus tremuloides* Michx.) and ponderosa pine (*Pinus ponderosa* Dougl. Ex Laws). Both aspen (deciduous broad-leaf, fast-growing) and ponderosa pine (evergreen conifer, slow-growing) are ecologically important and two of the most widespread tree species in North America. In the southwestern United States, aspen grows across a variety of habitats and reproduces asexually from root suckering. Ponderosa pine also grows in diverse climates from wind-dispersed seed but typically at sites with more moisture-limited soil than aspen. Both species have experienced drought-induced mortality events in recent decades (Ganey & Vojta, 2011; Worrall et al., 2008).

Study plots were established in natural forest stands in the San Juan National Forest (SJNF) of Southwest Colorado, USA. Plots span the lower transition of arid piñon-juniper woodland to ponderosa pine forest (~2,320 m) to the upper transition of montane aspen forest to fir-spruce forest (~3,080 m), and were established as 18-m radius, circular plots (0.10-ha plots) in mature aspen and ponderosa pine stands at the lower elevation range margin (low), range center (mid) and upper elevation range margin (high) of each species. Plots were randomly established within elevation zones within 1 km of a road and selected to maintain relatively consistent slopes and aspects to avoid microtopographic variation. In the SJNF, approximately 50% of precipitation occurs during winter and 50% during summer monsoons that begin in mid- to late-July, resulting in peak water stress in late June/early July (Anderegg et al., 2013).

Plots were visited 29 June–9July in 2014, 27 June–10 July in 2018, and 24 June–29 June in 2019 for data collection. The same focal trees were sampled every year unless the tree had died, in which case they were replaced with nearby similar trees. Diameter at breast height (DBH) was measured on the focal trees in 2014 and on all trees in the plots with DBH > 4 cm in 2018. In 2019, percent canopy dieback (mortality) was visually estimated for all trees in the plots with DBH > 4 cm. Permission was not needed for fieldwork. See Tables S1 and S5 for more information regarding numbers of plots and sample sizes used for this study.

Geographic plot centers (Trimble Geo 7x; Trimble, Inc.) were used to extrapolate monthly climatic variables of interest at ~4 km spatial resolution from 1958 to 2019 (TerraClimate; Abatzoglou et al., 2018): maximum temperature (T_{max}, °C), vapour pressure deficit (VPD, kPa), precipitation accumulation (PPT, mm), climate water deficit (mm) and Palmer Drought Severity Index (PDSI) (See SI Methods for more information regarding climatic variables). Monthly snow depth (cm) and snow water equivalent (SWE, cm) from 2005 to 2019 were obtained from the nearest snow telemetry site (SNOTEL site number 1060, Natural Resources Conservation Service).

2.2 | Xylem tension

Xylem tension measurements were made on distal twigs from all focal trees before sunrise (predawn, 03:00–05:30) and during midday (13:00–15:00), which reflects soil moisture limitation and the maximum tension a tree experiences, respectively, in a given 24-hr period (Ritchie & Hinckley, 1975). Branches were collected from sun-exposed, south-facing parts of mid-to-upper canopies with a 20-gauge shotgun. Twigs were recut from fallen branches >10 cm distance from the branch break, and xylem tensions were immediately measured on 1–3 twigs per tree with a Scholander-type pressure chamber (PMS Instruments). Predawn xylem tensions in high-elevation aspen plots during 2018 were not measured because of forest fires that restricted access to these plots.

2.3 | Hydraulic measurements

One large sun-exposed, south-facing, mid-to-upper canopy branch (diameter ~ 5–10 cm) was collected from each focal tree using a 20-gauge shotgun during midday. Collected branches were immediately placed into plastic bags with the branch break wrapped in a wet paper towel and placed into a cooler for transport back to the laboratory. Most samples were processed in the laboratory ~1–2 days after collection (~4% of samples required re-measuring but were not processed beyond 5 days after collection, a timeframe that has been used for both deciduous (Hacke & Sauter, 1996) and coniferous species (Lachenbruch et al., 2021)).

Branch segments were cut under water using a sharp razor blade to produce sample segments with sapwood diameters of ~5 mm and lengths of ~10 cm to accommodate tracheid and vessel lengths (Maherali & DeLucia, 2000; Sperry et al., 1991). Foliage distal to the cut segment was imaged with a fixed-distance digital camera (2014, 2018) or flatbed scanner (2019) to calculate projected leaf area using ImageJ (Schneider et al., 2012). Hydraulic conductance was measured using the pressure-flow method (Sperry et al., 1988) with a 2% potassium chloride 0.2 μm filtered solution. Native conductance (k_{nat}) was first measured, then samples underwent overnight vacuum infiltration to remove embolisms and determine maximum conductance (k_{max}). k_{nat} and k_{max} values were standardized by the sapwood area and length of the segment to determine native and maximum sapwood area-specific conductivity ($K_{s\text{-}nat}$ and $K_{s\text{-}max}$, respectively). k_{nat} values were also standardized by leaf area and length of the segment to determine native leaf area-specific conductivity ($K_{nat\text{-}Leaf}$). Problematic samples were screened (SI Methods) and percent loss of conductance (PLC), which represents the degree of embolism present in the sample, was quantified using Equation 1:

$$\text{PLC}(\%) = \left(\frac{k_{max} - k_{nat}}{k_{max}}\right) \times 100 \quad (1)$$

In 2019, a second branch sample was collected from focal trees and prepared as described above to produce stem sample segments with equivalent diameters and lengths. These samples were perfused with a 0.2 μM filtered 0.1% (mass/volume) safranin dye solution (Hacke & Sauter, 1996). Basal ends of the samples were immersed in the dye solution, and distal ends were fitted to a water-filled tubing manifold. Dye was pulled through the samples by lowering the free end of the manifold just below the dye surface creating a ~3 kPa pressure gradient. Samples were perfused until a sufficient 'cloud' of dye occurred in the water above the distal end, then were immediately rinsed and placed in a freezer until processing. Thin cross-sections were taken from the distal end of each stem ~7 cm away from the initial cut using a microtome and imaged with a microscope and camera (Nikon Eclipse e600; Nikon, Japan). Areas (mm^2) of stained (functional) and non-stained sapwood were analysed using ImageJ to calculate percent functional xylem in each sample.

2.4 | Morphological traits

SLA and leaf area to sapwood area ratios (A_L:A_S) were determined using the leaves/needles collected from the aspen and pine hydraulic stem samples. Total one-sided area of leaves/needles (A_L) was quantified with images (using a fixed-distance digital camera in 2014, 2018, or flatbed scanner in 2019) and ImageJ. After imaging, leaves/needles were dried in a 60°C oven and final dry weights were recorded using a mass balance (Sartorius, Germany). SLA was calculated by dividing A_L by dry weight. A_L:A_S was calculated by dividing A_L by the sapwood diameter at the basal end of the branch segment. When subtending foliage for a branch was very large, we quantified SLA on a randomly selected subset of leaves, and estimated whole-branch A_L by multiplying SLA by the total dry weight of all the foliage. SLA and A_L:A_S were also measured during the months of June (8–11 June) and August (13–18 August) of 2018 to investigate variation in these traits during the drought year.

A subset of dried foliage from the branches collected for hydraulic measurements were also used for carbon isotope discrimination (Δ). See SI Methods and Table S6 for carbon isotope discrimination methods and results.

2.5 | Pressure-volume parameters

Pressure-volume (PV) curve parameters were determined for focal trees in low- and high-elevation zones during 2018 and 2019. In the laboratory, small aspen twigs (diameter ~ 5–10 mm) or intact pine fascicle bundles with healthy, non-necrotic foliage were selected from the branches collected for hydraulic measurements. Twigs and fascicle bundles were excised from branches under water >10 cm distance from the branch break and underwent overnight rehydration. Portions of each sample that had been under water during rehydration were removed prior to measurement to minimize impacts of oversaturation on the shape of the P-V curve, known as the 'plateau effect' (Parker & Pallardy, 1987). As samples dried on the benchtop, water potential (Ψ) and weights to the nearest 0.0001 g were measured periodically, using a Scholander-type pressure chamber and mass balance, respectively. PV curve parameters were determined (Koide et al., 1989) including leaf turgor loss point (Ψ_{TLP}), the point at which leaf cells lost turgor; leaf osmotic potential at full turgor ($\Psi\pi_{100}$), the solute concentration in leaf cells at full hydration; and modulus of elasticity (ε), cell wall stiffness.

2.6 | Analyses

Linear mixed-effects models were constructed for each species to relate absolute xylem tension or trait values to the fixed effects of year, elevation and their interaction and random effects of either tree or plot to account for repeated measures. Model assumptions of normality for each model were checked by examining diagnostic plots of residuals, and data were transformed with log or square root transformations when assumptions were violated. Extreme outliers were determined using the Cook's Distance method and removed from the SLA and A_L:A_S datasets when necessary.

Both year (2014, 2018, 2019) and elevation (low, mid, high) were coded categorically, and appropriate random effect structure (tree or plot) was determined based on AIC and the full fixed model structure (Zuur et al., 2009). Final fixed model structure was then selected via Akaike information criterion (AIC) as the simplest model within 2 AIC of the lowest AIC model. The effects of year, elevation and their interaction were then determined with likelihood ratio tests (LRT) by comparing the full model with reduced models. When year or elevation proved to be significant, pairwise comparisons were made to test whether measurement values differed significantly across years within each elevation zone or across the elevation zones within individual years. Pairwise comparisons were made between groups using the estimated marginals means and the Tukey method for *p*-value adjustments.

We calculated spatial and temporal coefficients of variation (CV, standard deviation/mean) to quantify the extent of variation in the following drought response traits: A_L:A_S, $P_a - P_i$, $K_{s\text{-}max}$, $K_{nat\text{-}Leaf}$, SLA, and Ψ_{TLP}. For spatial CVs, we first determined mean values across years within each elevation zone (i.e. one value per elevation zone), and then calculated CV across the three elevation zones. For temporal CVs, we first determined mean values across the three elevation zones within each year (i.e. one value per year), and then calculated CV across the three years.

Linear regressions were used to investigate if drought response trait values predicted drought-induced tree mortality following the 2018 severe drought. Values for drought response traits (SLA, A_L:A_S, $P_a - P_i$, PLC, Ψ_{TLP}, $K_{nat\text{-}Leaf}$, $K_{s\text{-}max}$, and $K_{s\text{-}nat}$) were averaged by plot resulting in a single data point per plot per species. Coefficients of determination (R^2) and *p*-values were determined through linear regression of mean plot-level trait values against 2019 canopy dieback scores. Data points for both aspen SLA and A_L:A_S included potential outlier plots and analyses were done both with and without these plots.

Statistical analyses were conducted in R version 3.6.1 (R Core Team, 2021). The 'lme4' (version 1.1-21), 'lmerTest' (version 3.1-0) and 'emmeans' (version 1.4) packages were used to construct and analyse mixed-effects models (Bates et al., 2015; Kuznetsova et al., 2017; Lenth et al., 2022). Significance of fixed effects were determined with LRTs using 'lmerTest' and the Satterthwaite approximation method. Pairwise comparisons were determined using 'emmeans' and the Tukey method for *p*-value adjustments. The 'car' package (version 2.1.6) was used to plot QQ normal lines with 95% confidence intervals for assumption validation (Fox & Weisberg, 2018). For all analyses, significance levels of $\alpha < 0.05$ and $\alpha = 0.05$–0.1 were considered statistically significant and marginally significant, respectively. For graphical representations, we present bootstrapped means and confidence intervals (bootstrap replicates with replacement = 1,000) for relevant measurements.

3 | RESULTS

3.1 | Climate

Climate varied substantially in this study: 2014 was an average water year, 2018 a severe drought year and 2019 an above-average wet year (Table S2). In 2014, precipitation (PPT), maximum temperature (T_{max}), vapour pressure deficit (VPD), and snowpack closely matched historic mean values of each variable. In 2018, PPT and snowpack were below average while T_{max} and VPD were above average (Figure 1). The Palmer Drought Severity Index (PDSI) was −4.27 in June 2018, indicating that 2018 was one of driest years on record for the SJNF (Figure S2B). In 2019, the SJNF received above average PPT and one of the highest snowpack years on record the preceding winter (Figure S2A).

3.2 | Xylem tension

Xylem tension generally decreased with elevation, was highest during the severe drought of 2018 and was lowest during the wet year of 2019 for both species. Elevation significantly affected aspen xylem tension ($\chi^2 = 64.358$, $p < 0.0001$, Figure S3A) as low-elevation aspen generally had the highest predawn and midday xylem tensions. Low-elevation pine also had higher predawn and midday xylem tensions than high-elevation pines ($\chi^2 = 36.326$, $p < 0.0001$, Figure S3B), but elevation had a smaller effect for this species. Aspen predawn and midday xylem tensions were highest during 2018 and lowest during 2019 across all elevation zones, indicating that year was significant ($\chi^2 = 368$, $p < 0.0001$, Figure S3A). Similarly, pine midday xylem tensions were consistently highest during 2018, while both predawn and midday xylem tensions were lowest during 2019 across the elevation zones (effect of year: $\chi^2 = 398.92$, $p < 0.0001$, Figure S3B).

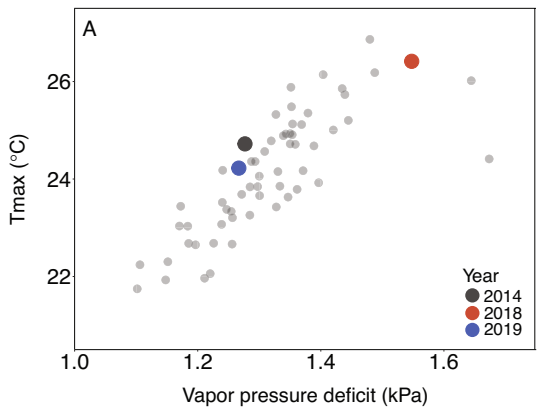

FIGURE 1 Atmospheric conditions varied across the study: 2014 was an average year, 2018 a severe drought year and 2019 an above-average wet year. Points reflect mean June maximum temperature (T_{max}) and vapour pressure deficit for all plots from 1958 to 2019 and coloured dots reflect study years. Data were generated from a 4 km gridded climate dataset (TerraClimate; Abatzoglou et al., 2018).

3.3 | Hydraulic measurements

There were species-specific spatial and temporal differences in hydraulic conductivity and native embolism, yet no significant differences in total percent of functional xylem measured in 2019 among the elevation zones for each species (Figure S4).

Aspen hydraulic measurements only varied temporally. In particular, the 2018 drought substantially reduced both native sapwood area-specific conductivity ($K_{s\text{-}nat}$) and maximum sapwood area-specific conductivity ($K_{s\text{-}max}$) in mid-elevation aspen (Figure 2a), although sample sizes were low (i.e. $N = 3$) due to logistical complications. The wet year of 2019 resulted in increased hydraulic conductivity: $K_{s\text{-}nat}$ was higher in 2019 compared with 2018 in mid-elevation aspen ($p = 0.0428$), and $K_{s\text{-}max}$ was significantly

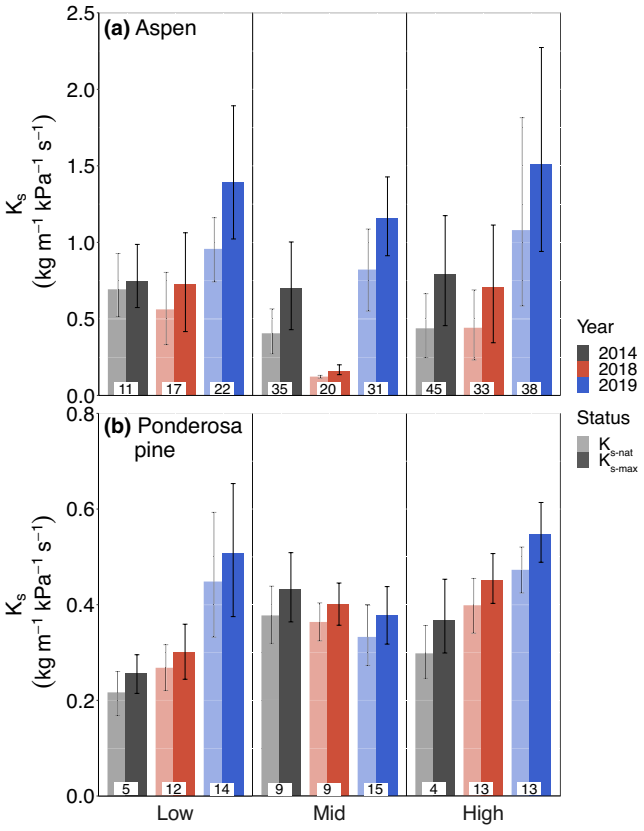

FIGURE 2 Native ($K_{s\text{-}nat}$) and maximum ($K_{s\text{-}max}$) sapwood area-specific conductivity showed species-specific differences in variation. (a) In aspen, mid-elevation ramets had reduced conductivity during the 2018 drought, while the 2019 wet year resulted in increased conductivity in all plots. Percent loss of conductance (PLC, number in white box) was unaffected by the 2018 drought and generally increased with increasing elevation. (b) In ponderosa pine, conductivity typically increased with increasing elevation and during the 2019 wet year. PLC was low (<20%) in all plots and did not vary across space or time. Bars represent bootstrapped means from all plots per elevation band for $K_{s\text{-}nat}$ (light bars) and $K_{s\text{-}max}$ (dark bars), and error bars represent bootstrapped 95% confidence intervals. Statistical results have been omitted from this figure to aid in visual interpretation (see Tables S3 and S4). Note: *y*-axes scales are species-specific.

highest during 2019 compared with 2018 in all aspen elevation zones (Figure 2a). In contrast, PLC among the aspen stands did not vary from year-to-year and appeared unaffected by the 2018 drought. PLC generally increased with increasing elevation ($\chi^2 = 23.238$, $p = 0.0007$) and (Figure 2a).

Pine exhibited more variation in hydraulic measurements than aspen. High-elevation pines had significantly higher conductivity values, indicating elevation significantly affected both $K_{s\text{-}nat}$ ($\chi^2 = 26.657$, $p = 0.0002$) and $K_{s\text{-}max}$ ($\chi^2 = 29.854$, $p < 0.0001$, Figure 2b). Conductivity values were also highest during the 2019 wet year among low- and high-elevation pines, indicating year significantly affected both $K_{s\text{-}nat}$ ($\chi^2 = 25.936$, p = 0.0002) and $K_{s\text{-}max}$ ($\chi^2 = 26.998$, $p = 0.0001$, Figure 2b). PLC was low (<20%) in all pine plots and showed very little variation in space and time (Figure 2b).

Native leaf area-specific conductivity ($K_{nat\text{-}Leaf}$) varied temporally in both species. Low-elevation aspen had significantly lower $K_{nat\text{-}Leaf}$ during the 2018 drought compared with 2014 ($p = 0.0393$) and 2019 ($p = 0.0196$, Figure 3a). In pine, $K_{nat\text{-}Leaf}$ was significantly highest during the climatically average year of 2014 compared with 2018 and 2019, indicating a significant year effect ($\chi^2 = 61.779$, $p < 0.0001$, Figure 3c). Differences in $K_{nat\text{-}Leaf}$ from year-to-year were likely partly driven by corresponding temporal differences in leaf area, where increased leaf area (i.e. higher leaf area to sapwood area ratios) resulted in decreased $K_{nat\text{-}Leaf}$.

3.4 | Morphological traits

Leaf area to sapwood area ratios (A_L:A_S) were significantly lowest during the climatically average year of 2014 for both species and all elevation zones (Figure 3b,d). 2018–2019 year-to-year variation in A_L:A_S was species-specific within the low-elevation stands: aspen A_L:A_S was significantly higher during the 2018 drought compared with the 2019 wet year ($p = 0.0014$, Figure 3b), while pine A_L:A_S was significantly lower during the 2018 drought compared with the 2019 wet year ($p = 0.005$, Figure 3d). In aspen, A_L:A_S also varied with elevation, where A_L:A_S was highest during the 2018 drought in low-elevation aspen compared with mid- ($p = 0.0075$) and high- ($p = 0.004$) elevation aspen, and lowest during the 2019 wet year in low-elevation aspen compared with mid ($p = 0.0106$) elevation aspen (Figure 3b). Therefore, the best model for A_L:A_S in aspen included a significant year × elevation interaction ($\chi^2 = 25.812$, $p < 0.0001$) in addition to significant year ($\chi^2 = 123.27$, $p < 0.0001$) and elevation ($\chi^2 = 29.642$, $p < 0.0001$) effects.

There was relatively low variation in SLA for either species. For aspen, differences in SLA were driven by a large increase in SLA during the 2019 wet year, particularly in high-elevation aspen (Figure S5A). For pine, differences in SLA were driven by consistently lower SLA in 2014 within the low- and mid-elevation zones (Figure S5B). Over the growing season of the 2018 drought year, SLA changed little in either species (Figure S6). A_L:A_S also showed little variation within 2018 for pine but did significantly decrease from July to August in low- and high-elevation aspen (Figure S7), due to either leaf shedding or continued branch xylem growth after leaf expansion.

3.5 | Pressure-volume parameters

Leaf water potential at the turgor loss point (Ψ_{TLP}) was a key drought response trait for both species. Ψ_{TLP} was significantly more negative during the 2018 drought in both low- and high-elevation aspen and in low-elevation aspen compared with high-elevation aspen during the 2019 wet year (Figure 4a,b). Therefore, the best model for Ψ_{TLP} in aspen included the significant effects of year ($\chi^2 = 64.598$, $p < 0.001$), elevation ($\chi^2 = 24.943$, $p < 0.001$) and year × elevation interaction ($\chi^2 = 19.225$, $p < 0.001$). Ψ_{TLP} was similarly less negative during the 2019 wet year than the 2018 drought in pine, with the largest differences between the years in high-elevation pine plots (Figure 4d). As a result, the best model for Ψ_{TLP} in pines included a significant year effect ($\chi^2 = 17.419$, $p = 0.0002$), a marginally significant elevation effect ($\chi^2 = 5.4685$, $p = 0.065$) and a significant year × elevation interaction ($\chi^2 = 4.7704$, $p = 0.029$).

Relationships between Ψ_{TLP} and leaf osmotic potential at full turgor ($\Psi\pi_{100}$) were generally significant ($p < 0.001$) in both species, which suggests that $\Psi\pi_{100}$ (i.e. osmotic adjustment) was likely an important driver of Ψ_{TLP}. The strongest relationships occurred within high-elevation aspen ($R^2 = 0.85$, $p < 0.001$, Figure 4b) and high-elevation pine ($R^2 = 0.81$, $p < 0.001$, Figure 4d) during the 2019 wet year. The weakest relationship occurred in low-elevation aspen during the 2018 drought ($R^2 = 0.002$, $p = 0.86$, Figure 4a), which suggests there may be a limit to the extent that Ψ_{TLP} can be adjusted via more negative $\Psi\pi_{100}$ in these ramets.

Relationships between Ψ_{TLP} and the modulus of elasticity (ε) were weak and only significant for aspen (Figure S8). The strongest relationship between the two variables occurred in high-elevation aspen during the 2019 wet year ($R^2 = 0.29$, $p = 0.03$), yet these results indicated cell wall stiffness increased with more negative Ψ_{TLP} (Figure S8A). The relationship between the two variables was marginally significant in low-elevation aspen during the 2018 drought ($R^2 = 0.19$, $p = 0.067$), which suggests ε may have also been an important driver of Ψ_{TLP} for these aspens (Figure S8A).

3.6 | Carbon isotope discrimination

Larger differences in partial pressures of atmospheric and leaf intercellular CO_2 (i.e. higher $P_a - P_i$) indicate increased drawdown of leaf intercellular CO_2 due to either reduced stomatal conductance (g_s) with constant photosynthesis (A), or increased A with constant g_s (or some combination thereof). Low-elevation aspen exhibited higher $P_a - P_i$ (Figure S9A) and lower foliar nitrogen (Figure S10A) compared with high-elevation aspen ($\chi^2 = 33.089$, $p < 0.0001$) regardless of year, which suggests low-elevation aspen ramets likely have higher water use efficiency (A/g_s) due to reduced g_s and not increased photosynthetic capacity. In addition, all aspen exhibited

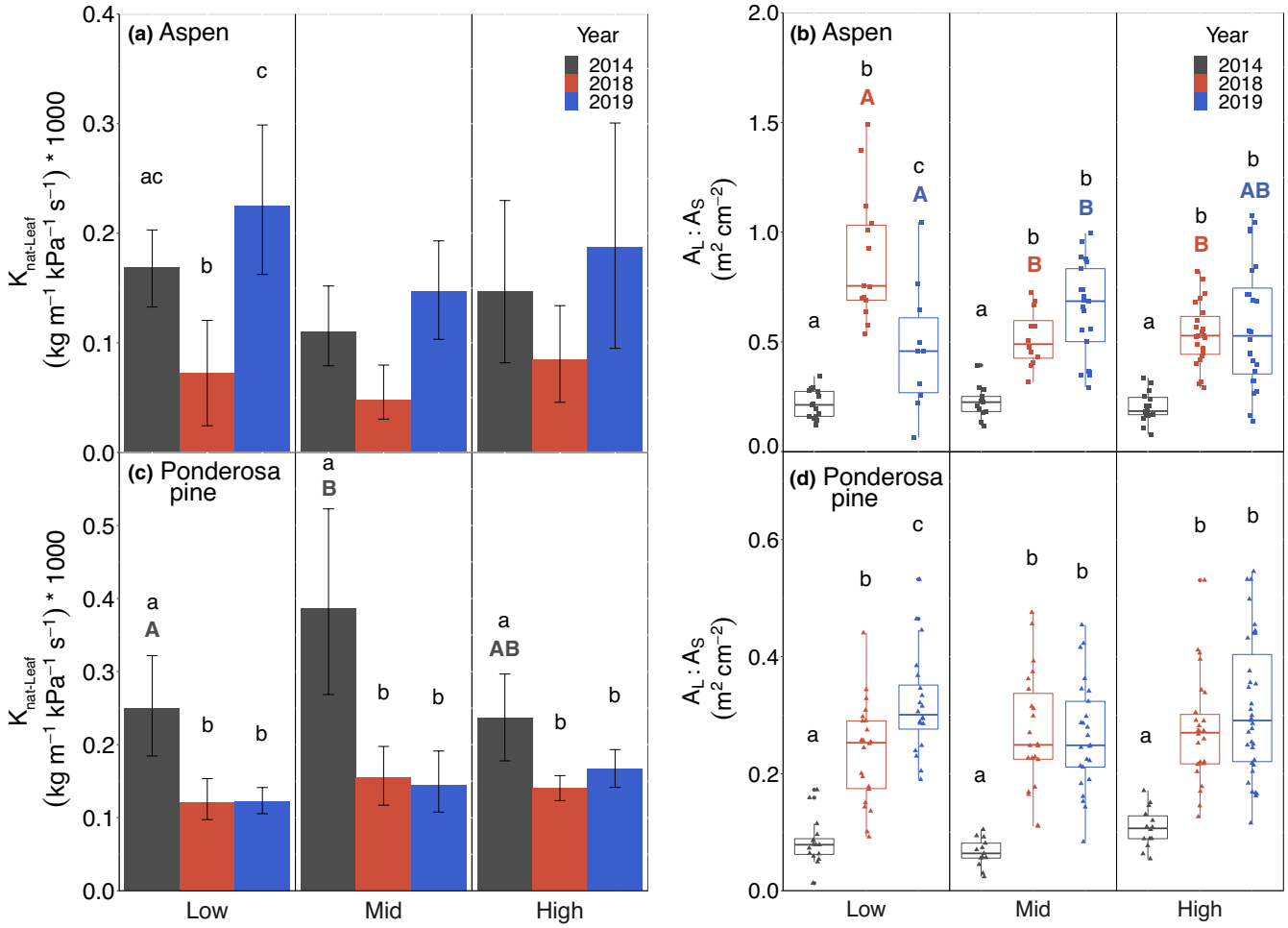

FIGURE 3 Year-to-year variation in leaf area affected native leaf area-specific conductivity ($K_{nat\text{-}Leaf}$) and leaf area to sapwood area ratios (A_L:A_S). In aspen, (a) $K_{nat\text{-}Leaf}$ was lowest during the 2018 drought while (*b*) A_L:A_S was higher, particularly in low-elevation aspen. Higher $K_{nat\text{-}Leaf}$ with high A_L:A_S during the 2019 wet year was likely due to more favourable environmental conditions for sapwood growth that year. In ponderosa pine, (c) $K_{nat\text{-}Leaf}$ was lowest during both the 2018 drought and 2019 wet year when (d) A_L:A_S was highest. Bars represent bootstrapped means from all plots per elevation band for $K_{nat\text{-}Leaf}$, and error bars represent bootstrapped 95% confidence intervals. Boxplots with tree-level observations are scattered within each boxplot for aspen (squares) and pine (triangles) and represent median A_L:A_S (center bar), interquartile range (IQR, edges of box), values at most 1.5 × IQR from box edge (error bars) and outlying points (circular points). Significant differences across years within a single elevation zone are indicated by lowercase black letters. Significant differences across elevation zones within a single year are indicated by bold, uppercase letters where font colour reflects the year of comparison. Significant results have unique letters while nonsignificant results share the same letters. Certain nonsignificant results have been omitted from this figure to aid in visual interpretation (Tables S3 and S4).

significantly higher $P_a - P_i$ during 2018 and 2019 compared with 2014 ($p < 0.0001$).

3.7 | Spatial versus temporal variation

Drought response traits in both species universally exhibited more temporal than spatial variation as reflected by comparisons of spatial and temporal coefficients of variation (CVs). Temporal variation was particularly high for A_L:A_S and $K_{nat\text{-}Leaf}$ in both species, as well as $K_{s\text{-}max}$ in aspen (Figure 5). In addition to universally large temporal variation, the magnitude of trait CVs was similar between aspen and pine for A_L:A_S, Ψ_{TLP}, and SLA, but aspen had larger spatial and temporal CVs for $P_a - P_i$ and $K_{nat\text{-}Leaf}$ and larger temporal variation in $K_{s\text{-}max}$.

3.8 | Relationships with drought-induced tree mortality

Pine suffered little to no canopy dieback during the 2018 drought, resulting in no significant drought response trait-mortality relationships (Figure S11). Aspen, however, suffered considerable canopy dieback in 2019 and aspen with higher SLA ($p = 0.002$, $R^2 = 0.71$ or $p = 0.04$, $R^2 = 0.47$ with outlier high mortality plot removed) and $P_a - P_i$ ($p = 0.029$, $R^2 = 0.58$) during the 2018 drought experienced increased canopy dieback during 2019 (Figure 6). Aspen with higher A_L:A_S during the 2018 drought also experienced increased canopy dieback in 2019, but this relationship was only marginally significant (Figure 6, $p = 0.0862$, $R^2 = 0.36$ with removal of the high A_L:A_S plot which only consisted of one focal tree).

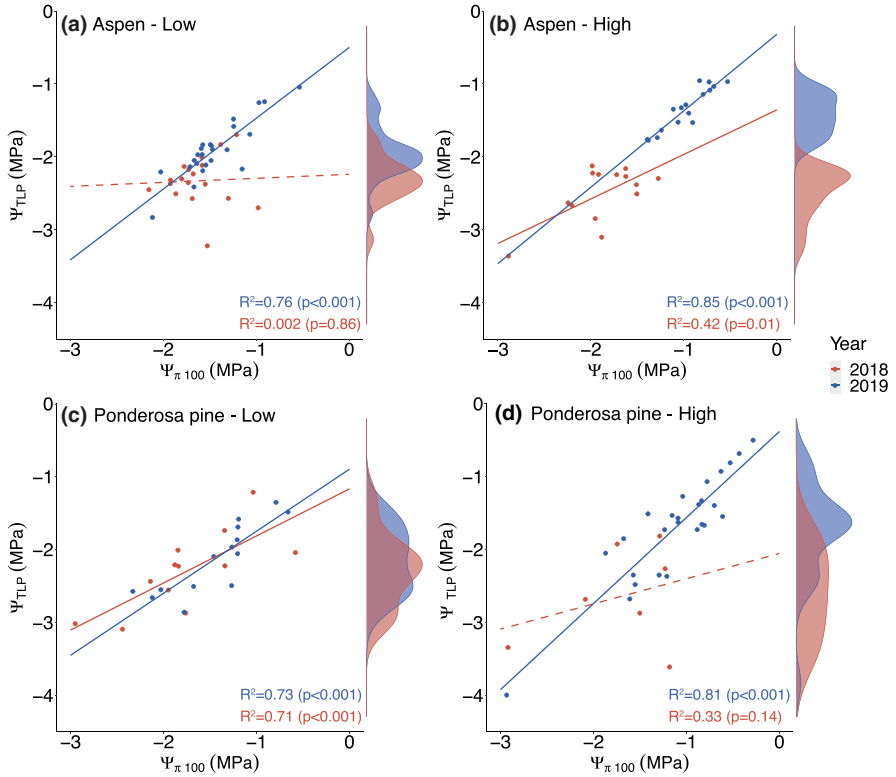

FIGURE 4 Regressions between leaf water potential at the turgor loss point (Ψ_{TLP}) and leaf osmotic potential at full turgor ($\Psi\pi_{100}$) suggest that osmotic adjustment was likely an important driver of Ψ_{TLP}. In aspen, regression was (a) weakest in low-elevation ramets during the 2018 drought and (b) strongest in high-elevation ramets during the 2019 wet year. (a, b) Margins: Ψ_{TLP} was significantly more negative during the 2018 drought in both low- and high-elevation aspen, and at low elevation during the 2019 wet year. In ponderosa pine, regression was (c) similar across both years in low-elevation trees and (d) stronger in high-elevation trees during the 2019 wet year. (c, d) Margins: Ψ_{TLP} was significantly more negative during the 2018 drought in high-elevation pine. Points represent tree-level observations and lines (solid = significant regression fits, dashed = non-significant regression fits) represent linear model regression fits (R^2 and *p*-values from linear models are printed on each figure). Marginal histograms represent Ψ_{TLP} values for 2018 and 2019 in the low and high plots for each species. [Correction added on 12 July 2022, after first online publication: Figure 4 has been revised].

4 | DISCUSSION

Quantifying trait variation across space and time revealed substantial drought response trait variation in our focal species, but many traits showed strong limits to plasticity and few traits showed correlation with mortality patterns. Both aspen and pine exhibited more temporal trait variation than spatial variation in every trait, highlighting the large potential for plasticity even on short timescales (year-to-year). In both species, differences in leaf area production were a major underlying factor in tree growth and physiology under the various climatic conditions observed in this study. In addition, leaf water potential at the turgor loss point (Ψ_{TLP}) was an important trait for increased drought tolerance in both species, but particularly for aspen. However, aspen at the low, dry range margin of this species appeared to be functioning at their drought tolerance threshold during the drought year which may indicate a limit to the extent that Ψ_{TLP} can be adjusted to further improve drought tolerance. Overall, canopy dieback following the severe drought was highest in low-elevation aspen stands and significantly correlated with increased SLA.

[Correction added on 12-July-22, after first online publication, revised supplementary file has been updated]

4.1 | Spatial variation in drought response traits

Both aspen and pine trees experienced elevated levels of drought stress at their lower, drier range margins as reflected by higher predawn and midday xylem tensions, indicating that soil moisture becomes limited at these species' low-elevation boundaries. A previous 1-year study at this site found that low-elevation aspen had denser wood and leaves and more embolism-resistant xylem, while pine showed little variation in those traits (Anderegg & HilleRisLambers, 2016). Here, we discovered that low-elevation aspen ramets had more negative turgor loss points (Ψ_{TLP}) and potentially higher water-use efficiency compared with their high-elevation counterparts, which reflects the higher drought tolerance of these low-elevation aspen that frequently experience drought stress (Bartlett et al., 2012; Ehleringer, 1993).

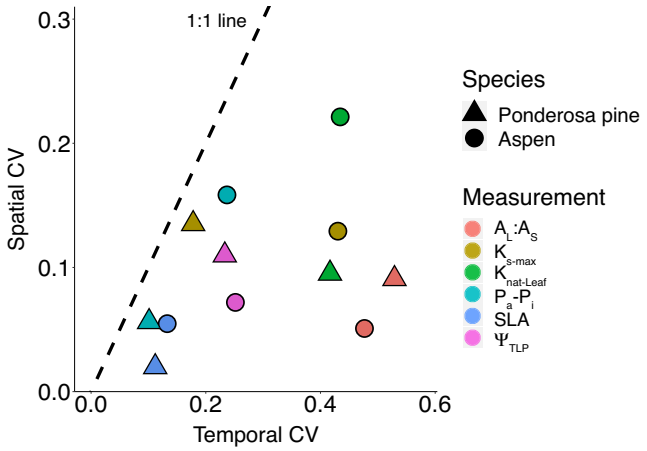

FIGURE 5 Drought response measurements exhibited more temporal variation, particularly for leaf area to sapwood area ratios (A_L:A_S) and native leaf area-specific conductivity ($K_{nat\text{-}Leaf}$). Points reflect temporal and spatial coefficients of variation (CV) for A_L:A_S, maximum sapwood area-specific conductivity ($K_{s\text{-}max}$), $K_{nat\text{-}Leaf}$, partial pressures of atmospheric and leaf intercellular CO_2 ($P_a - P_i$), specific leaf area (SLA), and leaf water potential at the turgor loss point (Ψ_{TLP}) in both species.

Aspen growing at the low-elevation boundary likely have higher drought tolerance due to decreased Ψ_{TLP} in these ramets, a well-documented drought tolerance trait (Bartlett et al., 2012). More negative Ψ_{TLP} and osmotic potential at full turgor ($\Psi\pi_{100}$), and strong correlations between the two, suggest that osmotic adjustment was likely the mechanism underlying decreases in Ψ_{TLP}. Osmotic adjustment consists of the accumulation of solutes in leaf cells to promote turgor maintenance and plant growth during periods of low water availability (Morgan, 1984). Another mechanism is elastic adjustment or an increase in leaf cell wall flexibility (i.e. decreasing the modulus of elasticity, ε). Elastic adjustments may have also contributed to decreased Ψ_{TLP} in low-elevation aspen as the correlation between Ψ_{TLP} and ε in these trees was marginally significant (Figure S8), suggesting low-elevation aspen ramets with more elastic leaf cell walls may also be more drought tolerant.

PLC showed consistent spatial patterns across the aspen plots and was higher with increasing elevation in any given year. Due to the inherently hotter and drier conditions that occur at the lower, drier range margin for this species, we expected to see higher PLC in low-elevation aspen due to the increased risk of cavitation under higher xylem tensions (Sperry & Tyree, 1988). These counter-intuitive

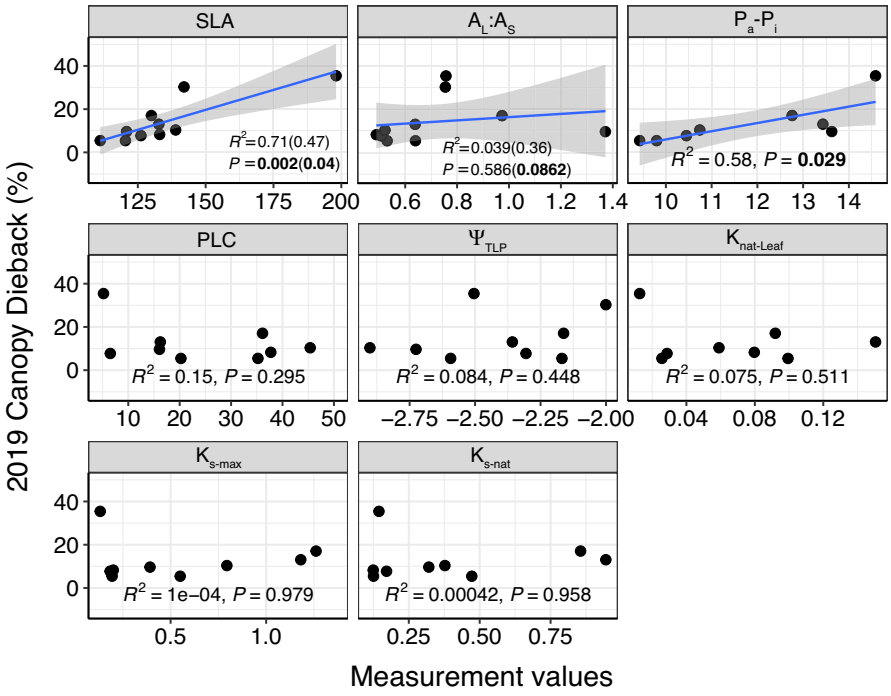

FIGURE 6 Aspen with higher specific leaf area (SLA), leaf area to sapwood area ratios (A_L:A_S), and partial pressures of atmospheric and leaf intercellular CO_2 ($P_a - P_i$) during the 2018 drought experienced increased canopy dieback (mortality) in 2019. Points represent plot-level mean values, the blue line represents significant linear model regression fit (R^2 and p-values from linear models are printed on each figure), and shaded areas represent 95% confidence intervals. Results for SLA remain significant even after removal of the high mortality plot, while results for A_L:A_S were marginally significant after removal of the high A_L:A_S plot (R^2 and p-value without these plots are in parentheses). Drought response measurements include SLA, A_L:A_S, $P_a - P_i$, percent loss of conductance, leaf water potential at the turgor loss point (Ψ_{TLP}), native leaf area-specific conductivity ($K_{nat\text{-}Leaf}$), maximum sapwood area-specific conductivity ($K_{s\text{-}max}$), and native sapwood area-specific conductivity ($K_{s\text{-}nat}$).

results may be due to the occurrence of freeze–thaw events during the winter in the high-elevation aspen plots. Aspen in Utah have been shown to be vulnerable to winter embolism due to freeze–thaw cycles in the xylem sap (Sperry et al., 1994). However, increased winter embolism does not seem to necessarily result in increased mortality the following spring, as Utah aspen maintained equivalent rates of leaf-area specific hydraulic conductivity as other angiosperm species during the subsequent growing season (Sperry et al., 1994). Indeed, in our study leaf-area specific conductivity varied considerably year-to-year but was quite similar across elevations in each year despite the consistent elevational differences in PLC. PLC values were lower in pine and did not show the same elevational trend as seen in aspen, which is likely due to species-specific differences in xylem anatomy. Ponderosa pine produce tracheid cells with smaller volumes and thicker cell walls, resulting in xylem that is more resistant to embolism (Hacke & Sperry, 2001).

4.2 | Temporal variation (phenotypic plasticity) in drought response traits

Nearly all the drought response traits exhibited some temporal variation across the scope of this study for both species (Figure 5). In addition, there was much more temporal trait variation than spatial variation which could have been due to larger variation in annual climate than elevation (Dwyer et al., 2014). Because the same focal trees were typically used across the years, the genotype of each individual tree/ramet was held constant which indicates both aspen and pine have acclimation potential and were capable of considerable phenotypic plasticity in response to environmental change. While many of the drought response traits did respond to the different climatic conditions of each individual year as we would expect, some of the responses were counter-intuitive that seemed to be driven by temporal differences in leaf production among years.

Xylem area-specific hydraulic conductivities were highest during 2019 for most aspen and pine, suggesting there was no permanent damage from the 2018 drought due to increased xylem tension and cavitation events that would prevent water flow, or that there was growth of new functional xylem in 2019 to support water flow (Tyree & Zimmermann, 2002). In nearly all study plots, Ψ_{TLP} was more negative during the 2018 drought compared with the other years, suggesting our focal trees can plastically adjust Ψ_{TLP} to cope with and acclimate to more arid environmental conditions (Bartlett et al., 2014). However, given the weak correlations between Ψ_{TLP} and ε, and Ψ_{TLP} and $\Psi\pi_{100}$, in low-elevation aspen during 2018, and that Ψ_{TLP} values were comparable with the maximum water stress these aspen experienced (i.e. midday xylem tensions), our results indicate there are limitations in the extent to which osmotic or elastic adjustment can improve drought tolerance in low-elevation aspen during severe drought.

Ratios of leaf area to sapwood area (A_L:A_S) and leaf area-specific native conductivity ($K_{nat\text{-}Leaf}$) showed the greatest amounts of temporal variation for both species. In addition, A_L:A_S values during the 2018 drought year were equivalent to or higher than A_L:A_S values during the 2019 wet year due to the production of more leaf area. This increase in leaf area was unexpected given the hot and dry environmental conditions of 2018 and may have been due to autumnal climatic conditions during vegetative bud set the previous growing season or advanced phenology during 2018 due to warmer spring temperatures (Gordo & Sanz, 2010). The production of more leaf area in 2018 appeared to be mal-adaptive for aspen, as individuals with higher leaf area (i.e. increased A_L:A_S) suffered marginally significant higher rates of mortality following the drought, likely indicating a 'structural overshoot' (Jump et al., 2017). In contrast, pine with higher leaf area did not have elevated mortality following the drought. However, ponderosa pine retain needles for 2–9 years (Ewers & Schmid, 1981) and the burden of increased leaf area from 2018 may result in future physiological consequences for these trees. We observed a decrease in aspen A_L:A_S when it was remeasured later in 2018 (Figure S7A), which suggests sapwood growth was not complete during the July measurement or that leaf shedding occurred. This seasonal dynamic highlights that intra-annual variability in growth and physiology may play an important role in fully understanding intraspecific functional trait variation.

Phenotypic plasticity has been documented for drought response traits in both aspen (St. Clair et al., 2010) and ponderosa pine (Maherali et al., 2002). Populations at species' range edges have also been shown to exhibit more trait plasticity which may help them deal with the more extreme environmental conditions at these boundaries (López et al., 2016; Stojnić et al., 2017). Though we cannot identify the driver of differential plasticity across elevations in this study (i.e. genotype vs. environment), it is noteworthy that half of all trait models included an elevation by year interaction which indicates a high degree of intraspecific functional trait variation within our study plots. Improved knowledge of intraspecific functional trait variation is integral for improving our ability to model forest responses to climate change, and long-term monitoring studies could provide excellent research opportunities to further assess the importance of phenotypic plasticity in trait variation for tree species as well as the severity and timing of drought as underlying factors in plastic responses.

4.3 | Predicting drought-induced tree mortality

We did not find many significant relationships between functional trait measurements made during the severe drought in 2018 and canopy dieback in 2019 (Figure 6; Figure S11). We hypothesize that this may be in part due to lags between drought and tree mortality. In general, mortality was still relatively low in 2019 yet delayed mortality of up to 4–10 years following drought has been documented for aspen in this region (Worrall et al., 2010) and in many tree species around the globe (Trugman et al., 2018). It is likely that substantial drought-induced mortality triggered by the 2018 drought will continue to play out in the San Juan National Forest during the next 5–10 years.

Aspen ramets with higher SLA (i.e. more leaf area per unit dry mass) and A_L:A_S (i.e. more leaf area per sapwood area) during the 2018 drought year had more canopy dieback in 2019. These data agree with other studies where leaves with higher SLA tend to be thinner, larger, and more sensitive to drought (Greenwood et al., 2017). In addition, trees with higher A_L:A_S may be the result of a 'structural overshoot' where increased above-ground biomass is not supported by available water, resulting in strong growth reductions and the onset of drought-induced mortality (Jump et al., 2017). Monitoring how functional traits influence mortality, as well as the potential shifts in functional trait composition associated with tree mortality, is of the utmost importance for improving our ability to forecast forest responses to climate change.

AUTHORS' CONTRIBUTIONS

The experiment was designed by all authors. Data collection and analyses were carried out by L.D.L.A., K.L.K. and N.Z., while data interpretation was carried out by all authors. K.L.K. led the writing of the manuscript, and all authors contributed to drafts and gave final approval for publication.

ACKNOWLEDGEMENTS

The authors thank Jaycee Cappaert, Shelby Jenkins, Coleson Kastelic, Elizabeth Schattle, Sophie Buyesse, Grayson Badgley, Anna Trugman, Martin Venturas, Dan Ott, Beth Blattenberger, Bryce Alex, Mary Beninati and Michaela Lemen for their assistance with field and laboratory work. K.L.K. acknowledges support from the University of Utah Global Change and Sustainability Center and the University of Utah Rio Mesa Center. L.D.L.A. acknowledges support from NSF Grant 1711243 and 2003205. N.Z. acknowledges support from the NSF Graduate Research Fellowship Program Grant No. 1747505. W.R.L.A. acknowledges funding from the David and Lucille Packard Foundation, NSF Grants 1714972, 1802880 and 2003017, and the USDA National Institute of Food and Agriculture, Agricultural and Food Research Initiative Competitive Programme, Ecosystem Services and Agro-ecosystem Management, Grant no. 2018-67019-27850.

CONFLICT OF INTEREST

The authors do not declare any conflicts of interest.

DATA AVAILABILITY STATEMENT

Data available from the Dryad Digital Repository https://doi.org/10.5061/dryad.v6wwpzgzn (Kerr et al., 2022).

ORCID

Kelly L. Kerr https://orcid.org/0000-0002-0830-2148
Leander D. L. Anderegg https://orcid.org/0000-0002-5144-7254
Nicole Zenes https://orcid.org/0000-0002-4126-7794
William R. L. Anderegg https://orcid.org/0000-0001-6551-3331

REFERENCES

Abatzoglou, J. T., Dobrowski, S. Z., Parks, S. A., & Hegewisch, K. C. (2018). TerraClimate, a high-resolution global dataset of monthly climate and climatic water balance from 1958–2015. *Scientific Data*, *5*, 1–12. https://doi.org/10.1038/sdata.2017.191

Adams, H. D., Macalady, A. K., & Breshears, D. D. (2010). Climate-induced tree mortality: Earth system consequences. *Eos*, *91*(17), 153–154.

Aitken, S. N., Yeaman, S., Holliday, J. A., Wang, T., & Curtis-McLane, S. (2008). Adaptation, migration or extirpation: Climate change outcomes for tree populations. *Evolutionary Applications*, *1*(1), 95–111. https://doi.org/10.1111/j.1752-4571.2007.00013.x

Albert, C. H., Thuiller, W., Yoccoz, N. G., Douzet, R., Aubert, S., & Lavorel, S. (2010). A multi-trait approach reveals the structure and the relative importance of intra- vs. interspecific variability in plant traits. *Functional Ecology*, *24*(6), 1192–1201. https://doi.org/10.1111/j.1365-2435.2010.01727.x

Anderegg, L. D. L., & HilleRisLambers, J. (2016). Drought stress limits the geographic ranges of two tree species via different physiological mechanisms. *Global Change Biology*, *22*(3), 1–9. https://doi.org/10.1111/gcb.13148

Anderegg, W. R. L. (2015). Spatial and temporal variation in plant hydraulic traits and their relevance for climate change impacts on vegetation. *New Phytologist*, *205*(3), 1008–1014. https://doi.org/10.1111/nph.12907

Anderegg, W. R. L., Anderegg, L. D. L., & Huang, C.-Y. (2019). Testing early warning metrics for drought-induced tree physiological stress and mortality. *Global Change Biology*, *25*(7), 2459–2469. https://doi.org/10.1111/gcb.14655

Anderegg, W. R. L., Plavcová, L., Anderegg, L. D. L., Hacke, U. G., Berry, J. A., & Field, C. B. (2013). Drought's legacy: Multiyear hydraulic deterioration underlies widespread aspen forest die-off and portends increased future risk. *Global Change Biology*, *19*(4), 1188–1196. https://doi.org/10.1111/gcb.12100

Bartlett, M. K., Scoffoni, C., & Sack, L. (2012). The determinants of leaf turgor loss point and prediction of drought tolerance of species and biomes: A global meta-analysis. *Ecology Letters*, *15*(5), 393–405. https://doi.org/10.1111/j.1461-0248.2012.01751.x

Bartlett, M. K., Zhang, Y., Kreidler, N., Sun, S., Ardy, R., Cao, K., & Sack, L. (2014). Global analysis of plasticity in turgor loss point, a key drought tolerance trait. *Ecology Letters*, *17*(12), 1580–1590. https://doi.org/10.1111/ele.12374

Bates, D., Mächler, M., Bolker, B., & Walker, S. (2015). Fitting linear mixed-effects models using lme4. *Journal of Statistical Software*, *67*(1), 1–48. https://doi.org/10.18637/jss.v067.i01

Borghetti, M., Gentilesca, T., Leonardi, S., Van Noije, T., & Rita, A. (2017). Long-term temporal relationships between environmental conditions and xylem functional traits: A meta-analysis across a range of woody species along climatic and nitrogen deposition gradients. *Tree Physiology*, *37*(1), 4–17. https://doi.org/10.1093/treephys/tpw087

Dai, A. (2013). Increasing drought under global warming in observations and models. *Nature Climate Change*, *3*(1), 52–58. https://doi.org/10.1038/nclimate1633

Dodd, R. S., & Douhovnikoff, V. (2016). Adjusting to global change through clonal growth and epigenetic variation. *Frontiers in Ecology and Evolution*, *4*(JUL), 1–6. https://doi.org/10.3389/fevo.2016.00086

Dwyer, J. M., Hobbs, R. J., & Mayfield, M. M. (2014). Specific leaf area responses to environmental gradients through space and time. *Ecology*, *95*(2), 399–410. https://doi.org/10.1890/13-0412.1

Ehleringer, J. R. (1993). Carbon and water relations in desert plants: An isotopic perspective. In *Stable isotopes and plant carbon–water relations*. Academic Press, Inc. https://doi.org/10.1016/b978-0-08-091801-3.50018-0

Ewers, F. W., & Schmid, R. (1981). Longevity of needle fascicles of *Pinus longaeva* (Bristlecone pine) and other North American pines. *Oecologia*, *51*(1), 107–115. https://doi.org/10.1007/BF00344660

Fox, J., & Weisberg, S. (2018). *An R companion to applied regression* (3rd ed.). Sage Publications.

Ganey, J. L., & Vojta, S. C. (2011). Tree mortality in drought-stressed mixed-conifer and ponderosa pine forests, Arizona, USA. *Forest Ecology and Management*, *261*(1), 162–168. https://doi.org/10.1016/j.foreco.2010.09.048

Gordo, O., & Sanz, J. J. (2010). Impact of climate change on plant phenology in Mediterranean ecosystems. *Global Change Biology*, *16*(3), 1082–1106. https://doi.org/10.1111/j.1365-2486.2009.02084.x

Greenwood, S., Ruiz-Benito, P., Martínez-Vilalta, J., Lloret, F., Kitzberger, T., Allen, C. D., Fensham, R., Laughlin, D. C., Kattge, J., Bönisch, G., Kraft, N. J. B., & Jump, A. S. (2017). Tree mortality across biomes is promoted by drought intensity, lower wood density and higher specific leaf area. *Ecology Letters*, *20*(4), 539–553. https://doi.org/10.1111/ele.12748

Hacke, U., & Sauter, J. J. (1996). Xylem dysfunction during winter and recovery of hydraulic conductivity in diffuse-porous and ring-porous trees. *Oecologia*, *105*(4), 435–439. https://doi.org/10.1007/BF00330005

Hacke, U., & Sperry, J. S. (2001). Functional and ecological Xylem anatomy. *Perspectives in Plant Ecology, Evolution and Systematics*, *4*(2), 97–115.

Jump, A. S., Ruiz-Benito, P., Greenwood, S., Allen, C. D., Kitzberger, T., Fensham, R., Martínez-Vilalta, J., & Lloret, F. (2017). Structural overshoot of tree growth with climate variability and the global spectrum of drought-induced forest dieback. *Global Change Biology*, *23*(9), 3742–3757. https://doi.org/10.1111/gcb.13636

Kerr, K. L., Anderegg, L. D. L., Zenes, N., & Anderegg, W. R. L. (2022). Quantifying within species trait variation in space and time reveals limits to trait-mediated drought response. *Dryad Digital Repository*, https://doi.org/10.5061/dryad.v6wwpzgzn

Koide, R. T., Robichaux, R. H., Morse, S. R., & Smith, C. M. (1989). Plant water status, hydraulic resistance and capacitance. In R. W. Pearcy, J. R. Ehleringer, H. A. Mooney, & P. H. Rundel (Eds.), *Plant physiological ecology* (pp. 161–183). Springer. https://doi.org/10.1007/978-94-009-2221-1_9

Kuznetsova, A., Brockhoff, P. B., & Christensen, R. H. B. (2017). lmerTest package: Tests in linear mixed effects models. *Journal of Statistical Software*, *82*(13), 1–26.

Lachenbruch, B., St. Clair, J. B., & Harrington, C. A. (2021). Differences in branch hydraulic architecture related to the aridity of growing sites and seed sources of coastal Douglas-fir saplings. *Tree Physiology*, *42*(2), 351–364. https://doi.org/10.1093/treephys/tpab106

Lenth, R. V. (2022). emmeans: Estimated marginal means, aka least-squares means. *CRAN Repository*. https://CRAN.R-project.org/package=emmeans

López, R., Cano, F. J., Choat, B., Cochard, H., & Gil, L. (2016). Plasticity in vulnerability to cavitation of pinus canariensis occurs only at the driest end of an aridity gradient. *Frontiers in Plant Science*, *7*(June), 1–10. https://doi.org/10.3389/fpls.2016.00769

Maherali, H., & DeLucia, E. H. (2000). Xylem conductivity and vulnerability to cavitation of ponderosa pine growing in contrasting climates. *Tree Physiology*, *20*(13), 859–867.

Maherali, H., Williams, B. L., Paige, K. N., & Delucia, E. H. (2002). Hydraulic differentiation of Ponderosa pine populations along a climate gradient is not associated with ecotypic divergence. *Functional Ecology*, *16*(4), 510–521. https://doi.org/10.1046/j.1365-2435.2002.00645.x

Maherali, H., Pockman, W. T., & Jackson, R. B. (2004). Adaptive variation in the vulnerability of woody plants to zylem cavitation. *Ecology*, *85*(8), 2184–2199. https://doi.org/10.1890/02-0538

Martínez-Vilalta, J., Cochard, H., Mencuccini, M., Sterck, F., Herrero, A., Korhonen, J. F. J., Llorens, P., Nikinmaa, E., Nolè, A., Poyatos, R., Ripullone, F., Sass-Klaassen, U., & Zweifel, R. (2009). Hydraulic adjustment of Scots pine across Europe. *New Phytologist*, *184*(2), 353–364. https://doi.org/10.1111/j.1469-8137.2009.02954.x

McCulloh, K. A., & Sperry, J. S. (2005). Patterns in hydraulic architecture and their implications for transport efficiency. *Tree Physiology*, *25*(3), 257–267. https://doi.org/10.1093/treephys/25.3.257

McGregor, I. R., Helcoski, R., Kunert, N., Tepley, A. J., Gonzalez-Akre, E. B., Herrmann, V., Zailaa, J., Stovall, A. E. L., Bourg, N. A., McShea, W. J., Pederson, N., Sack, L., & Anderson-Teixeira, K. J. (2021). Tree height and leaf drought tolerance traits shape growth responses across droughts in a temperate broadleaf forest. *New Phytologist*, *231*(2), 601–616. https://doi.org/10.1111/nph.16996

Morgan, J. M. (1984). Osmoregulation and water stress in higher plants. *Annual Review of Plant Physiology*, *35*(1), 299–319. https://doi.org/10.1146/annurev.pp.35.060184.001503

Parker, W. C., & Pallardy, S. G. (1987). The influence of resaturation method and tissue type on pressure-volume analysis of *Quercus alba* L. seedlings. *Journal of Experimental Botany*, *38*(3), 535–549. https://doi.org/10.1093/jxb/38.3.535

R Core Team. (2021). *R: A language and environment for statistical computing*. R Foundation for Statistical Computing.

Ritchie, G. A., & Hinckley, T. M. (1975). The pressure chamber as an instrument for ecological research. *Advances in Ecological Research*, *9*(C), 165–254. https://doi.org/10.1016/S0065-2504(08)60290-1

Schneider, C. A., Rasband, W. S., & Eliceiri, K. W. (2012). NIH Image to ImageJ: 25 years of image analysis. *Nature Methods*, *9*(7), 671–675. https://doi.org/10.1038/nmeth.2089

Sperry, J. S., Donnelly, J. R., & Tyree, M. T. (1988). A method for measuring hydraulic conductivity and embolism in xylem. *Plant, Cell and Environment*, *11*, 35–40.

Sperry, J. S., Nichols, K. L., Sullivan, J. E. M., & Eastlack, S. E. (1994). Xylem embolism in ring-porous, diffuse-porous, and coniferous trees of northern Utah and interior Alaska. *Ecology*, *75*(6), 1736–1752.

Sperry, J. S., Perry, A. H., & Sullivan, J. E. M. (1991). Pit membrane degradation and air-embolism formation in ageing xylem vessels of *Populus tremuloides* Michx. *Journal of Experimental Botany*, *42*(11), 1399–1406.

Sperry, J. S., & Tyree, M. T. (1988). Mechanism of water stress-induced xylem embolism. *Plant Physiology*, *88*(3), 581–587. https://doi.org/10.1104/pp.88.3.581

Sperry, J. S., Venturas, M. D., Todd, H. N., Trugman, A. T., Anderegg, W. R. L., Wang, Y., & Tai, X. (2019). The impact of rising CO_2 and acclimation on the response of US forests to global warming. *Proceedings of the National Academy of Sciences of the United States of America*, *116*(51), 25,734–25,744. https://doi.org/10.1073/pnas.1913072116

St. Clair, S. B., Mock, K. E., LaMalfa, E. M., Campbell, R. B., & Ryel, R. J. (2010). Genetic contributions to phenotypic variation in physiology, growth, and vigor of Western Aspen (*Populus tremuloides*) Clones. *Forest Science*, *56*(2), 222–230.

Stojnić, S., Suchocka, M., Benito-Garzón, M., Torres-Ruiz, J. M., Cochard, H., Bolte, A., Cocozza, C., Cvjetković, B., de Luis, M., Martinez-Vilalta, J., Ræbild, A., Tognetti, R., & Delzon, S. (2017). Variation in xylem vulnerability to embolism in European beech from geographically marginal populations. *Tree Physiology*, *38*(February), 1–13. https://doi.org/10.1093/treephys/tpx128

Trugman, A. T., Detto, M., Bartlett, M. K., Medvigy, D., Anderegg, W. R. L., Schwalm, C., Schaffer, B., & Pacala, S. W. (2018). Tree carbon allocation explains forest drought-kill and recovery patterns. *Ecology Letters*, *21*(10), 1552–1560. https://doi.org/10.1111/ele.13136

Tyree, M. T., & Zimmermann, M. H. (2002). *Xylem structure and the ascent of sap* (2nd ed.; T. E. Timell, Ed.). Springer-Verlag.

Violle, C., Reich, P. B., Pacala, S. W., Enquist, B. J., & Kattge, J. (2014). The emergence and promise of functional biogeography. *Proceedings of the National Academy of Sciences of the United States of America*, *111*(38), 13,690–13,696. https://doi.org/10.1073/pnas.1415442111

Williams, A. P. A., Cook, E. E. R., Smerdon, J. J. E., Cook, B. I. B., Abatzoglou, J. J. T., Bolles, K., Baek, S. H., Badger, A. M., & Livneh,

B. (2020). Large contribution from anthropogenic warming to an emerging North American megadrought. *Science*, *368*(April), 314–318. https://doi.org/10.1126/science.aaz9600

Worrall, J. J., Egeland, L., Eager, T., Mask, R. A., Johnson, E. W., Kemp, P. A., & Shepperd, W. D. (2008). Rapid mortality of Populus tremuloides in southwestern Colorado, USA. *Forest Ecology and Management*, *255*(3–4), 686–696. https://doi.org/10.1016/j.foreco.2007.09.071

Worrall, J. J., Marchetti, S. B., Egeland, L., Mask, R. A., Eager, T., & Howell, B. (2010). Effects and etiology of sudden aspen decline in southwestern Colorado, USA. *Forest Ecology and Management*, *260*(5), 638–648. https://doi.org/10.1016/j.foreco.2010.05.020

Wright, I. J., Reich, P. B., Westoby, M., Ackerly, D. D., Baruch, Z., Bongers, F., Cavender-Bares, J., Chapin, T., Cornelissen, J. H. C., Diemer, M., Flexas, J., Garnier, E., Groom, P. K., Gulias, J., Hikosaka, K., Lamont, B. B., Lee, T., Lee, W., Lusk, C., … Villar, R. (2004). The worldwide leaf economics spectrum. *Nature*, *428*(6985), 821–827. https://doi.org/10.1038/nature02403

Zuur, A. F., Ieno, E. N., Walker, N. J., Saveliev, A. A., & Smith, G. M. (2009). *Mixed effects models and extensions in ecology with R*. Springer.

SUPPORTING INFORMATION

Additional supporting information can be found online in the Supporting Information section at the end of this article.

How to cite this article: Kerr, K. L., Anderegg, L. D. L., Zenes, N., & Anderegg, W. R. L. (2022). Quantifying within-species trait variation in space and time reveals limits to trait-mediated drought response. *Functional Ecology*, *36*, 2399–2411. https://doi.org/10.1111/1365-2435.14112